Available online at www.sciencedirect.com
SCIENCE DIRECT
Catalysis Today 111 (2006) 322–327
CATALYSIS TODAY
www.elsevier.com/locate/cattod

Different support effect of M/ZrO_2 and M/CeO_2 (M = Pd and Pt) catalysts on CO adsorption: A periodic density functional study

Changho Jung [a], Hideyuki Tsuboi [a], Michihisa Koyama [a,*], Momoji Kubo [a,b], Ewa Broclawik [c], Akira Miyamoto [a,c]

[a] *Department of Applied Chemistry, Graduate School of Engineering, Tohoku University, 6-6-07 Aoba, Aramaki, Aoba-ku, Sendai 980-8579, Japan*
[b] *PRESTO, Japan Science and Technology Agency, 4-1-8 Honcho, Kawaguchi, Saitama 332-0012, Japan*
[c] *New Industry Creation Hatchery Center, Tohoku University, 6-6-10 Aoba, Aramaki, Aoba-ku, Sendai 980-8579, Japan*

Available online 27 December 2005

Abstract

CO adsorption over Pd_4 and Pt_4 cluster supported by c-ZrO_2(1 1 1) and CeO_2(1 1 1) catalyst systems was investigated using periodic density functional method in order to clarify the support effect on CO activation. We found that the support increases the CO activation for bridge and three-fold sites but decreases for the atop site. Moreover, it was found that the support changes the site preference for the CO adsorption. Bridge site on both the Pt_4/c-ZrO_2 and Pt_4/CeO_2 show larger CO adsorption energies than those on the other sites while the atop site is energetically preferable on isolated Pt_4 cluster. c-ZrO_2 supported Pd shows the largest CO activation with large charge transfer from the catalyst to the CO molecule. This reveals that ZrO_2 supported Pd can be a good catalyst for CO activation because of its higher probability to the three-fold site CO adsorption. We also found that positively charged M_4 clusters on the support keep their strong electron-donating properties and have enough charge density to contribute to the activation of an adsorbed CO molecule by a charge transfer.

Keywords: CO adsorption; Precious metal; Support effect; Density functional theory

1. Introduction

CO adsorption on precious metal surfaces is one of the most prototypical catalytic reactions and hence, has been studied with various experimental [1–7] and theoretical [8–17] methods. On the other hand, precious metals such as Rh, Pd and Pt are the essential ingredients for the so-called three-way catalyst (TWC), which simultaneously decreases the amount of the exhaust pollutants, viz., CO, HCs (hydrocarbons) and NO_x. High dispersion of precious metal particles on the support is important for the enhancement of the catalytic activity as well as for the reduction in the economic cost of catalyst materials. Various metal oxide supports have been utilized for the preparation of well-dispersed supported metal catalysts. In this regard, it is noteworthy that zirconia (ZrO_2) and ceria (CeO_2) have been increasingly used for catalyst support [18–22]. Zirconia exhibits three well-defined crystal polymorphs, the monoclinic (m), tetragonal (t) and cubic (c) phases; it has also been shown that a high-pressure orthorhombic form exists. The high temperature cubic phase can be stabilized at room temperature by doping divalent cations such as Ca^{2+}, Mg^{2+} or trivalent Y^{3+}, and the stabilized zirconia has been extensively studied both theoretically and experimentally due to its wide technological applications [23,24]. Moreover, among the numerous precious metal supported catalyst systems, the metal supported zirconia attracts special attention because of the stability under wide temperature range [25]. On the other hand, CeO_2 is also widely used as a support of the TWC for stabilizing the precious metal particles. In addition, CeO_2 is known to enhance the TWC activity because of its oxygen storage capacity (OSC) [20–22]. The OSC is amplified by the metal/CeO_2 interactions leading to increase in the catalytic activity of the TWC [20]. However, it is difficult to characterize the geometric and electronic interactions of the metal/ZrO_2 and metal/CeO_2 interfaces by experiment because of their complexity.

In recent years, computational methods have become a powerful research tool for providing information at the atomic

* Corresponding author. Tel.: +81 22 795 7233; fax: +81 22 795 7235.
E-mail address: miyamoto@aki.che.tohoku.ac.jp (M. Koyama).

0920-5861/$ – see front matter © 2005 Elsevier B.V. All rights reserved.
doi:10.1016/j.cattod.2005.10.057

and electronic level. In particular, the density functional theory (DFT) calculations provide accurate energetic and electronic properties of materials including heavy metals.

At this juncture, it is important to mention that only very few theoretical studies have been performed for CO adsorption on supported precious metal catalysts whereas CO adsorption on clean metal surfaces such as Pt(1 1 1) has been discussed by many previous works. In this paper, we present the results for the CO adsorption on Pd_4 and Pt_4 clusters supported by c-ZrO_2(1 1 1) and CeO_2(1 1 1) catalyst systems using the periodic density functional method.

2. Method

Periodic DFT calculations were performed by solving the Kohn–Sham equations self-consistently [26] as implemented in the DMol^3 software [27]. One-electron equations were solved at Γ point of the Brillouin-zone. In order to reduce computational costs, all core electrons were represented by effective core pseudopotentials (ECP) [27]. In this study the double numerical with polarization (DNP) basis set was employed. Vosko–Wilk–Nusair (VWN) local correlation functional [28] was used in order to optimize geometries. Generalized gradient approximation (GGA) in terms of Perdew-Wang91 functional [29] was used for energy evaluation. For geometry optimization, BFGS algorithm [27] was employed. The self-consistent field convergence criterion was set to 10^{-5} Ha, while the gradient convergence was set to 10^{-3} Ha/Bohr. Charge population was analyzed using the Hirshfeld method. Geometries were optimized with thermal occupancies (with 0.005 a.u. window) while final energies were calculated with Fermi occupancies. Adsorption energies (E_{ads}) were calculated from energy difference between the optimized geometry of the CO/M_4/support system and optimized M_4/support plus the energy of the isolated CO molecule:

$$E_{ads} = E_{tot}(CO/M_4/support) - E_{tot}(M_4/support) + E_{tot}(CO)$$

3. Results and discussion

In the present study, (1 1 1) surfaces of cubic ZrO_2 (c-ZrO_2) and CeO_2 are employed, because this is the most stable surface for ceria and zirconia [30–32]. *O*-Terminated c-ZrO_2(1 1 1) and CeO_2(1 1 1) model surfaces with 6 atomic layers consisting of 8 metal atoms and 16 oxygen atoms were constructed for the present purpose. The simulation cell dimension for c-ZrO_2(1 1 1) and CeO_2 (1 1 1) surfaces were fixed to: $a = 6.21$ Å, $b = 7.17$ Å, $\alpha = \beta = \gamma = 90^\circ$ and $a = 6.63$ Å, $b = 7.65$ Å, $\alpha = \beta = \gamma = 90^\circ$, respectively. A pseudo-vacuum was applied along the *c*-axis (10 Å) on all surface models. Pt_4 and Pd_4 clusters were deposited on the c-ZrO_2(1 1 1) and CeO_2(1 1 1) surfaces. Geometry optimization calculations were performed for the M_4/c-ZrO_2(1 1 1) and M_4/CeO_2(1 1 1) (M = Pt and Pd) including surface relaxation of the oxide supports. Using the optimized M_4/oxide structures, we performed CO adsorption calculations on three different adsorption sites on the M_4/c-ZrO_2(1 1 1) and M_4/CeO_2(1 1 1), i.e. atop, bridge and three-fold sites of M_4. Geometry optimization calculations for the CO adsorption allowed for the relaxation of both the M_4 cluster and the oxide supports, except the fixed single bottom layer of the support. In addition, we also performed the CO adsorption calculations on the isolated M_4 clusters in order to compare these results with those on the supported systems.

There are many previous works on CO adsorption on clean Pt(1 1 1) and Pd(1 1 1) surfaces. CO adsorption energies of −32 to −35 kcal/mol were obtained on the Pt(1 1 1) surface by thermal desorption spectroscopy and light-induced thermal desorption method [3,4], whereas CO adsorption energies of −30 to −35 kcal/mol were obtained on the Pd(1 1 1) surface by thermal desorption spectroscopy method [5,6]. More recently, Yeo et al. reported −38 to −48 kcal/mol for the CO adsorption energy on the Pt(1 1 1) surface using single crystal adsorption calorimetry [7]. Moreover, experimental works indicate that CO prefers the atop site of the Pt(1 1 1) surface and the three-fold site of the Pd(1 1 1) surface. The above experimental adsorption energy values can be compared with our calculation results for the CO adsorption on the isolated M_4 clusters shown in Table 1. Site preference of CO obtained by our calculations is consistent with the above experimental works on both the Pt(1 1 1) and Pd(1 1 1) surfaces. However, the calculated adsorption energy of CO is larger than the experimental results. Previous DFT results for the CO adsorption on the Pt(1 1 1) surface also showed that the CO adsorption energy is larger than the experiments [17]. Moreover, Geschke et al. reported −53 kcal/mol for the adsorption energy of CO on Pt_{13} cluster, which is much larger than that for CO on the Pt(1 1 1) surface. These previous results suggest that a small cluster calculation provides a larger adsorption energy than experiments, which validates with our DFT results.

Optimized structures for the CO adsorption on the M_4/c-ZrO_2(1 1 1) and M_4/CeO_2(1 1 1) are shown in Figs. 1 and 2, respectively. Adsorption features of CO on the M_4/c-ZrO_2 and M_4/CeO_2 are summarized in Table 2. Adsorption energies on the supported M_4 clusters are shown in Fig. 3. In most cases, the CO adsorption energy values on the Pt_4 clusters are decreased when the clusters are supported on the c-ZrO_2(1 1 1) and CeO_2(1 1 1). An exception was observed for the CO adsorption on the bridge site of the Pt_4/c-ZrO_2(1 1 1). The site preference of the CO adsorption on the Pt_4 cluster was found to change when the clusters are supported on the c-ZrO_2(1 1 1) and CeO_2(1 1 1). Bridge sites on both the Pt_4/c-ZrO_2 and Pt_4/CeO_2

Table 1
CO adsorption features on the isolated Pt_4 and Pd_4 cluster

Cluster	Site	E_{ads} (kcal/mol)	*d*M–C (Å)	*d*C–O (Å)	*q*CO	*q*M_4
Pt_4	Atop	−61.4	1.808	1.159	−0.094	+0.094
	Bridge	−57.8	1.928, 1.931	1.185	−0.171	+0.171
	Three-fold	−52.9	1.988, 1.989, 2.004	1.211	−0.263	+0.263
Pd_4	Atop	−42.5	1.834	1.153	−0.142	+0.142
	Bridge	−44.8	1.874, 1.876	1.186	−0.271	+0.271
	Three-fold	−55.7	1.950, 1.950, 1.960	1.202	−0.366	+0.366

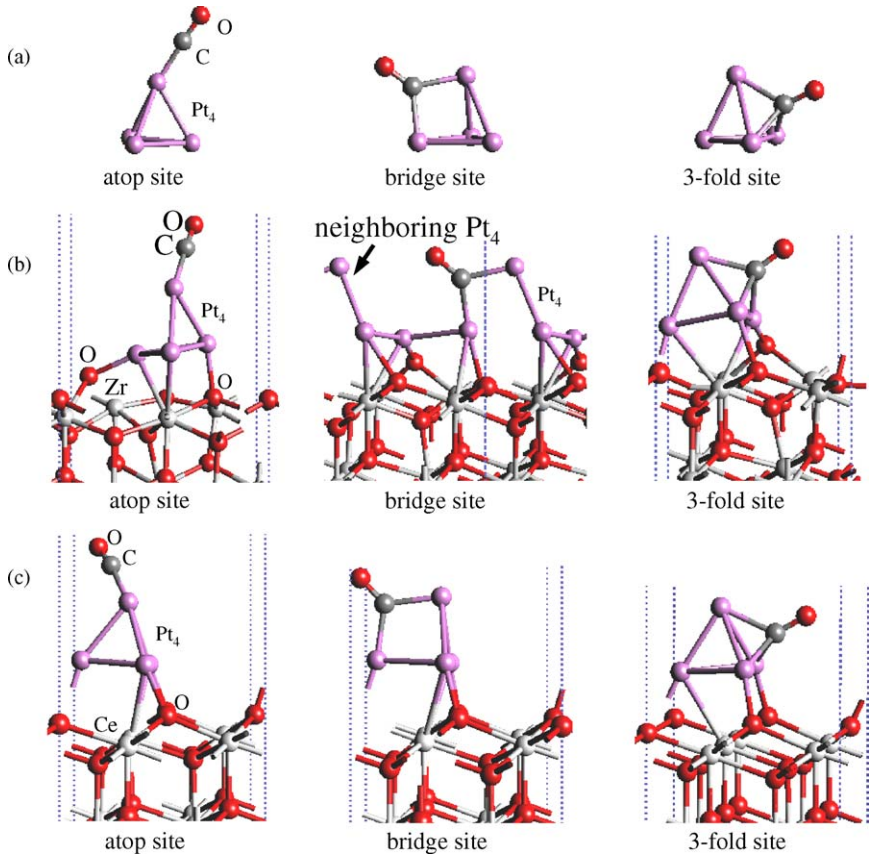

Fig. 1. Optimized structures for the CO adsorption on the isolated Pt_4 and supported Pt_4 cluster: (a) CO on the isolated Pt_4 cluster, (b) CO on the c-ZrO_2(1 1 1) supported Pt_4 cluster, (c) CO on the CeO_2(1 1 1) supported Pt_4 cluster.

show the larger CO adsorption energies than those on the other sites while CO adsorption on the isolated Pt_4 cluster prefers the atop site. The CO adsorption on both the Pd_4/c-ZrO_2 and Pd_4/CeO_2 also shows different site preference compared to that on the isolated Pd_4 cluster. The CO adsorption energy on the Pd_4 supported on the c-ZrO_2(1 1 1) and CeO_2(1 1 1) is comparable for the bridge and the three-fold sites while the CO prefers the three-fold site adsorption on the isolated Pd_4, which indicates a weaker site preference on support. Especially, a large increase in the CO adsorption energy was obtained for the bridge site. The CO adsorption energy on the three-fold site shows only a slight increase on the Pd_4/c-ZrO_2(1 1 1) compared to that on the isolated Pd_4 while a slight decrease is observed for the Pd_4/CeO_2(1 1 1). At the same time, the shift of the adsorption preference from the atop site to the bridge site indicates the large influence of the metal/support interactions on the CO adsorption. Comparison of the different support effects on the c-ZrO_2(1 1 1) and CeO_2(1 1 1) shows larger CO adsorption energy values on the M_4/c-ZrO_2(1 1 1) compared to those on the M_4/CeO_2(1 1 1). Our calculation results clearly show that a significant support effect on the CO adsorption can be observed on ultra-fine precious metal particle. On the other hand, we also found that the CO adsorption affects the geometry of the M_4 clusters. Fig. 4 shows the average M–M bond length of M_4 clusters. Increase in M–M interatomic distance was observed in all the calculated cases, and the c-ZrO_2(1 1 1) supported M_4 clusters show a larger increase in the Pt–Pt interatomic distance than the CeO_2(1 1 1) supported systems. Hence, we suggest that the larger geometrical relaxation of the c-ZrO_2(1 1 1) supported M_4 clusters contribute to the increase in the stability of CO adsorbed on the M_4/c-ZrO_2(1 1 1) compared to the CeO_2(1 1 1) supported systems.

In order to discuss CO activation, C–O bond lengths are also shown in Tables 1 and 2. CO shows much longer bond length on the bridge and three-fold site than that on the atop site in all the calculated cases (CO in gas phase equals to 1.13 Å in our DFT calculation). This reveals that the change in the site preference of the CO adsorption has important meaning not only for the strength of the M–CO binding but also for the activation of the C–O bond. C–O bond length on the atop site of the supported M_4 clusters is shorter compared to the atop site adsorption on the isolated M_4 clusters. The bridge site on the Pt_4/c-ZrO_2(1 1 1) and Pt_4/CeO_2(1 1 1) shows longer C–O bond lengths than that on the isolated Pt_4. three-fold site adsorption on the Pt_4/c-ZrO_2(1 1 1) and Pt_4/CeO_2(1 1 1) shows weaker support effect on the elongation of C–O bond compared to the bridge site adsorption. The Pd_4/c-ZrO_2(1 1 1) and Pd_4/CeO_2(1 1 1) shows weaker support effect on the elongation of C–O bond compared to the Pt_4/c-ZrO_2(1 1 1) and Pt_4/CeO_2(1 1 1) for the bridge site and three-fold site adsorption. Moreover, in the case of the bridge and three-fold site adsorption, longer C–O bond lengths were obtained on the c-ZrO_2(1 1 1) supported M_4 cluster compared to the CeO_2(1 1 1) supported systems, which means different support effect of the

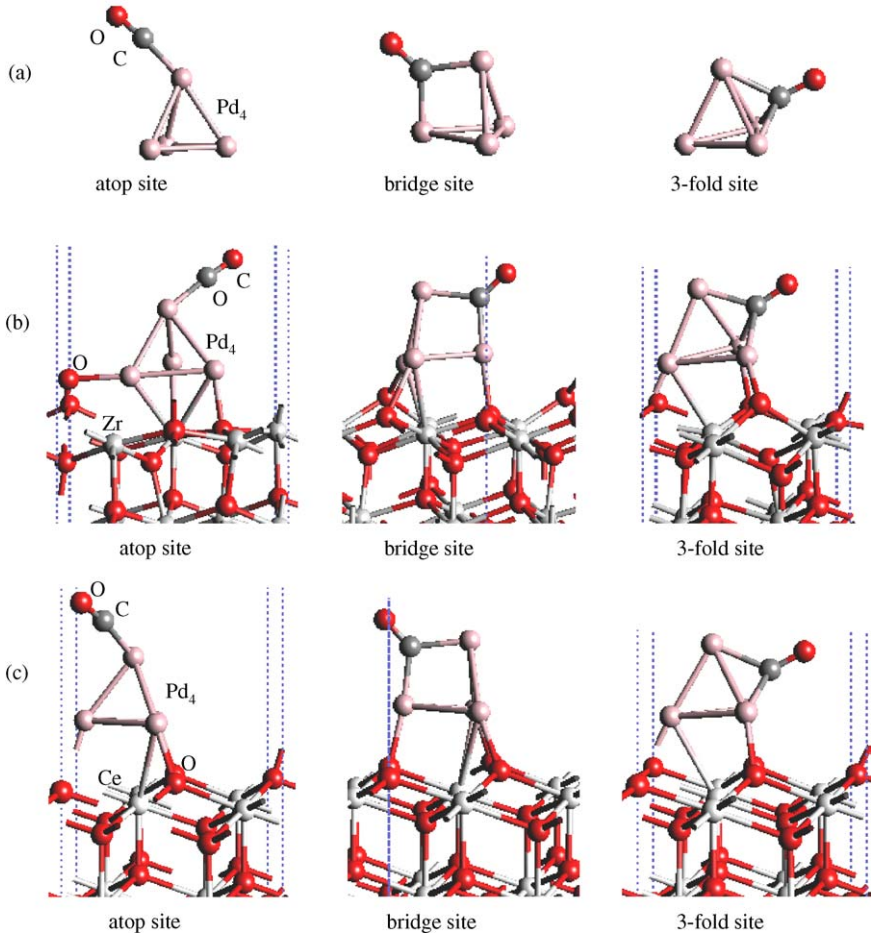

Fig. 2. Optimized structures for the CO adsorption on the isolated Pd_4 and supported Pd_4 cluster: (a) CO on the isolated Pd_4 cluster, (b) CO on the c-ZrO_2(1 1 1) supported Pd_4 cluster, (c) CO on the CeO_2(1 1 1) supported Pd_4 cluster.

c-ZrO_2(1 1 1) and CeO_2(1 1 1). On the other hand, the elongation of the C–O bond can be explained by the amount of negative charge on the adsorbed CO molecule. Fig. 5 shows the correlation between the C–O bond length and the negative charge of the CO molecule. It is well known that the LUMO of CO is an antibonding orbital (π^*), hence larger negative charge of CO molecule makes the C–O bond longer. Fig. 5 clearly indicates the strong correlation between the charge transfer and the CO bond length. The supported M_4 clusters have positive charge without CO adsorption in all the studied cases. M_4 clusters without CO have much larger positive charge on the CeO_2(1 1 1) compared to that on the c-ZrO_2(1 1 1), however the negative charge of CO shows almost the same value on both the M_4/c-ZrO_2(1 1 1) and M_4/CeO_2(1 1 1) models. In addition,

Table 2
CO adsorption features on the Pt_4 and Pd_4 clusters supported by the c-ZrO_2(1 1 1) and CeO_2(1 1 1)

Support	M_4	Site	dM–C (Å)	dC–O (Å)	qCO	qM$_4$	Δq of M_4	Δq of support	qM$_4$ without CO
ZrO_2	Pt_4	Atop	1.845	1.151	−0.030	+0.255	+0.027	+0.003	+0.228
		Bridge	1.922, 1.945	1.199	−0.195	+0.426	+0.198	−0.003	+0.228
		Three-fold	1.988, 2.030, 2.078	1.212	−0.228	+0.483	+0.255	−0.027	+0.228
	Pd_4	Atop	1.814	1.148	−0.077	+0.672	+0.232	−0.155	+0.440
		Bridge	1.874, 1.911	1.188	−0.293	+0.730	+0.290	+0.003	+0.440
		Three-fold	1.951, 1.987, 2.010	1.206	−0.366	+0.805	+0.365	+0.001	+0.440
CeO_2	Pt_4	Atop	1.876	1.152	−0.042	+0.338	+0.030	+0.012	+0.308
		Bridge	1.924, 1.945	1.196	−0.209	+0.532	+0.214	−0.005	+0.308
		Three-fold	2.027, 2.029, 2.050	1.207	−0.219	+0.504	+0.196	+0.023	+0.308
	Pd_4	Atop	1.858	1.150	−0.118	+0.634	+0.305	−0.187	+0.529
		Bridge	1.882, 1.909	1.186	−0.298	+0.829	+0.300	−0.002	+0.529
		Three-fold	1.967, 1.996, 1.996	1.202	−0.351	+0.877	+0.348	−0.003	+0.529

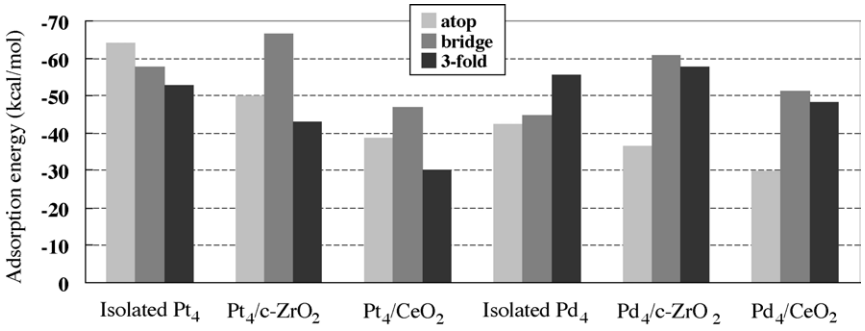

Fig. 3. Comparison of the CO adsorption energies between the isolated M_4 clusters and supported M_4 clusters.

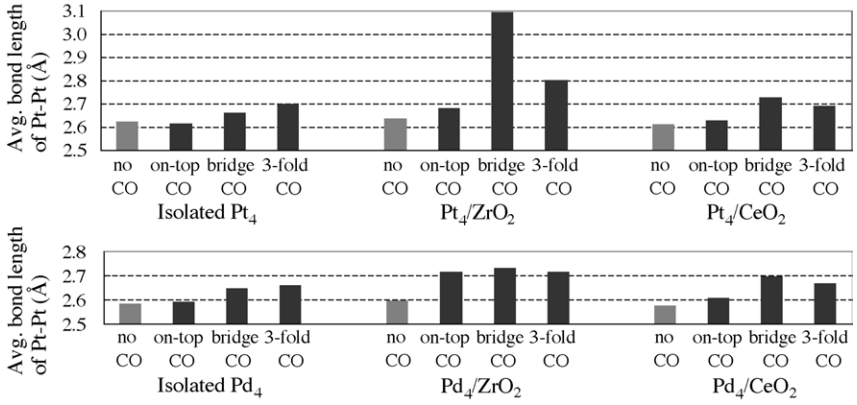

Fig. 4. Change in M–M bond lengths of the M_4 clusters by the CO adsorption.

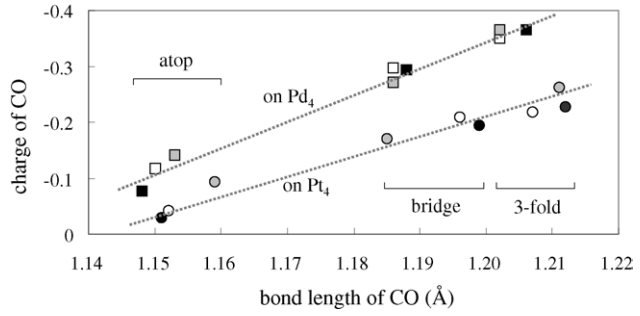

Fig. 5. Correlation between C–O bond length and charge of the CO molecule. Square marks indicate the results for Pd_4 cluster while circle marks indicate the results for Pt_4 cluster. Gray, black, and white colors indicate CO on the isolated M_4, CO on the c-ZrO_2(1 1 1) supported M_4, and CO on the CeO_2(1 1 1) supported M_4, respectively.

change in charge (Δq) of the support by the CO adsorption shown in Table 2 is small for all the calculated cases. This indicates that the positively charged M_4 clusters on the c-ZrO_2(1 1 1) and CeO_2(1 1 1) still have strong electron-donating properties and enough charge density to contribute to the activation of a single adsorbed CO molecule by charge transfer. Analysis of Fig. 5 illustrating relations between all the studied systems clearly indicates that the support effect is larger for Pt than for Pd, in particular for the bridge site. For the Pt systems smaller charge transfer is sufficient for the CO activation compared to the Pd systems. In addition, CO activation on the bridge site of supported Pt_4 cluster where the adsorption energy is the strongest, is comparable to that on the three-fold site showing weaker CO adsorption. On the other hand, three-fold site of supported Pd, that leads to high activation, shows only slightly lower adsorption energy than the bridge site. These results show that appropriate selection of the metal cluster with proper support leads to the development of new effective catalyst.

4. Conclusion

CO adsorptions over Pt_4 and Pd_4 clusters supported by c-ZrO_2(1 1 1) and CeO_2(1 1 1) were investigated using periodic density functional method in order to clarify the support effect on CO activation. Our results show that both the c-ZrO_2(1 1 1) and CeO_2(1 1 1) increase the CO activation for the bridge and three-fold sites but decreases the activation for the atop site. Moreover, the support changes the site preference for CO adsorption. CO prefers the bridge site on the supported Pt_4 cluster, while CO prefers the atop site on the isolated Pt_4 cluster. Moreover, the CO adsorption energy on Pd_4 supported on c-ZrO_2(1 1 1) and CeO_2(1 1 1) is comparable for the bridge and three-fold sites, which indicates less site preference. Larger CO adsorption energies were obtained for the c-ZrO_2(1 1 1) supported M_4 clusters compared to CeO_2(1 1 1) supported

M_4 clusters. This indicates that a significant support effect on the CO adsorption can be observed on ultra-fine precious metal particle. Moreover, the three-fold site is better than the bridge site for the CO activation in all the calculated cases. CO on the Pd_4/c-ZrO_2(1 1 1) shows only a slightly lower adsorption energy on the three-fold site than that on the bridge site whereas CO on the Pt_4/c-ZrO_2(1 1 1) shows much lower adsorption energy on the three-fold site than that on the bridge site. These two obtained results reveal that c-ZrO_2 supported Pd can be a good catalyst for CO activation because of its higher probability to the three-fold site CO adsorption. M_4 clusters on the c-ZrO_2(1 1 1) and CeO_2(1 1 1) have positive charge without CO adsorption in all the studied cases. The positively charged M_4 clusters on the c-ZrO_2(1 1 1) and CeO_2(1 1 1) were found to keep their strong electron-donating properties and have enough charge density to contribute to the activation of an adsorbed CO molecule.

References

[1] I. Langmuir, Trans. Faraday Soc. 17 (1921) 621.
[2] J. Wintterlin, S. Volkening, T.V.W. Jassens, T. Zambelli, G. Ertl, Science 278 (1997) 1931.
[3] H. Steininger, S. Lehwald, H. Ibach, Surf. Sci. 123 (1982) 264.
[4] E.G. Seebauer, A.C.F. Kong, L.D. Schmidt, J. Vac. Sci. Technol. A 5 (1987) 464.
[5] J. Szanyi, W.K. Kuhn, D.W. Goodman, J. Vac. Sci. Technol. A 11 (1987) 1969.
[6] X. Guo, J.T. Yates Jr., J. Chem. Phys. 90 (1989) 6761.
[7] Y.Y. Yeo, L. Vattuone, A. King, J. Chem. Phys. 106 (1) (1997) 392.
[8] S.A. Wasileski, M.T.M. Koper, M.J. Weaver, J. Phys. Chem. B 105 (2001) 3518.
[9] M.T.M. Koper, R.A. van Santen, J. Chem. Phys. 113 (2000) 8.
[10] X.Q. Gong, Z.P. Liu, R. Raval, P. Hu, J. Am. Chem. Soc. 126 (2004) 126.
[11] K. Doll, Surf. Sci. 573 (2004) 464.
[12] L. Kohler, G. Kresse, Phys. Rev. B 70 (2004) 165405.
[13] P. van Beurden, H.G.J. Verhoeven, G.J. Kramer, Phys. Rev. B 66 (2002) 235409.
[14] R.A. Olsen, P.H.T. Philipsen, E.J. Baerends, J. Chem. Phys. 119 (2003) 22.
[15] C.H. Jung, Y. Ito, H. Shibayama, A. Endou, M. Kubo, A. Imamura, A. Miyamoto, Trans. Mater. Res. Soc. Jpn. 29 (2004) 2181.
[16] D. Geschke, T. Bastug, T. Jacob, S. Fritzssche, W.D. Sepp, B. Fricke, Phys. Rev. B 64 (2001) 235411.
[17] M. Gajdoš, A. Eichler, J. Hafner, J. Phys.: Condens. Matter 16 (2004) 1141.
[18] R. Srinivasan, B.H. Davis, Catal. Lett. 14 (1992) 165.
[19] Z. Dang, B.G. Anderson, Y. Amenomiya, B.A. Morrow, J. Phys. Chem. 99 (1995) 14437.
[20] H.C. Yao, Y.F. Yu Yao, J. Catal. 86 (1984) 254.
[21] A. Trovarelli, Catal. Rev. Sci. Eng. 38 (1996) 439.
[22] J. Kaspar, P. Fornasiero, M. Graziani, Catal. Today 50 (1999) 285.
[23] E.V. Stefanovich, A.L. Shluger, C.R.A. Catlow, Phys. Rev. B 49 (17) (1994) 11560.
[24] G. Stapper, M. Bernasconi, N. Nicoloso, M. Parrinello, Phys. Rev. B 59 (1999) 797.
[25] J.H. Bitter, K. Seshan, J.A. Lercher, J. Catal. 171 (1997) 279; J.H. Bitter, K. Seshan, J.A. Lercher, J. Catal. 176 (1998) 93; J.H. Bitter, K. Seshan, J.A. Lercher, J. Catal. 183 (1999) 336.
[26] W. Kohn, L.J. Sham, J. Phys. Rev. A 140 (1965) 1133.
[27] DMol3 version 4.0, Accelrys, 1999.
[28] S.H. Vosko, L. Wilk, M. Nusair, Can. J. Phys. 58 (1980) 1200.
[29] J.P. Perdew, J.A. Chevary, S.H. Vosko, K.A. Jackson, M.R. Pederson, D.J. Singh, C. Fiolhais, Phys. Rev. B 46 (1992) 6671.
[30] S. Gennard, F. Cora, C.R.A. Catlow, J. Phys. Chem. B 103 (1999) 10158.
[31] A. Christensen, E.A. Carter, Phys. Rev. B 58 (1998) 8050.
[32] G. Balducci, J. Kaspar, P. Fornasiero, M. Graziani, M.S. Islam, J. Phys. Chem. B 102 (1998) 557.